

Detecting Defective Bypass Diodes in Photovoltaic Modules using Mamdani Fuzzy Logic System

Mahmoud Dhimish¹, Violeta Holmes² and Bruce Mehrdadi³

¹ University of Huddersfield

Received: 6 December 2016 Accepted: 2 January 2017 Published: 15 January 2017

Abstract

In this paper, the development of fault detection method for PV modules defective bypass diodes is presented. Bypass diodes are nowadays used in PV modules in order to enhance the output power production during partial shading conditions. However, there is lack of scientific research which demonstrates the detection of defective bypass diodes in PV systems. Thus, this paper propose a PV bypass diode fault detection classification based on Mamdani fuzzy logic system, which depends on the analysis of Vdrop, Voc , and Isc obtained from the I-V curve of the examined PV module. The fuzzy logic system depends on three inputs, namely percentage of voltage drop (PVD), percentage of open circuit voltage (POCV), and the percentage of short circuit current (PSCC). The proposed fuzzy system can detect up to 13 different faults associated with defective and non-defective bypass diodes. In addition, the proposed system was evaluated using two different PV modules under various defective bypass conditions. Finally, in order to investigate the variations of the PV module temperature during defective bypass diodes and partial shading conditions, i5 FLIR thermal camera was used.

Index terms— photovoltaic module, fault detection, fuzzy logic, thermal detection, bypass diodes.

1 INTRODUCTION

s prices in the photovoltaic (PV) industry have decreased considerably in the last few years, reliability questions have been proportional increased interest. The performance and efficiency of PV modules are affected by several factor such as solar irradiance, ambient temperature, humidity, and wind [1] [2] [3]. In addition, several work have studied and evaluated the performance of PV modules under different climate conditions, in particular the effect of sand dust accumulation and partial shading on the output power of PV modules and PV arrays [4 & 5].

In addition, PV modules output power performance could be decreased due to the PV cracks [6 & 7]. As reported in [8], PV cracks occur in PV solar cells due to partial shading conditions affecting some solar cells while the rest are under normal operation mode, also it might occur due to the dust and hot spots in PV modules. To solve this problem in PV modules, a bypass diodes connection to the PV strings is recommended.

As a result of these factors impacting the PV performance, a fault detection methods is indeed important to be employed and further investigate in PV systems. In general, fault detection method in PV systems can be grouped as visual (discoloration, surface soiling, and delamination), thermal (hot spots and PV micro cracks), and electrical (I-V, and P-V curve analysis, and transmittance line diagnosis) [9 & 10]. In this paper, we focus on an electrical method. Multiple PV fault detection based electrical methods for PV system are based on: 1. Methods do not require climate data (such as solar irradiance and PV module temperature). In [11] the authors developed a method based on the Earth Capacitance Measurements (ECM) to detect the disconnection of a PV module. The first Time-Domain Reflectometry (TDR) technique was proposed by [12]. This technique is used to detect the disconnection of PV strings as well as the impedance change due to PV degradation. Finally, [13][14][15] proposed a statistical analysis PV fault detection method based on t-test and standard deviation,

5 A) I-V CURVE CHARACTERISTICS UNDER PARTIAL SHADING CONDITIONS

44 which can be used to detect PV failure, and faults associated with maximum power point tracking (MPPT) units.
45 2. Methods based on the analysis of the current-voltage I-V characteristics. In [16], the analysis of the I-V and P-V
46 curve was used to investigate the performance of the PV module, thus, detecting possible faults such as partial
47 shading and faulty PV strings. In [17 & 18], the authors calculate the fill factor (FF), series resistance (R_s),
48 and the shunt resistance (R_{sh}) from the I-V curve to investigate the performance of multiple PV configuration
49 systems. Methods based on artificial intelligence (AI) techniques. In [19 & 20] the authors proposed a PV
50 fault detection algorithm which can identify the partial shading conditions in PV modules based on a fuzzy logic
51 system. However, the proposed technique cannot identify the impact of bypass diodes in PV modules, which
52 has been investigated by [21 & 22]. In addition, a learning method based on Expert Systems is developed by
53 [23][24][25] to identify faults in PV modules due to partial shading and inverter's failure. Furthermore, in [26],
54 an artificial neural network (ANN) is used in order to classify different types of faults occurring in a PV array. In
55 this case, the ANN takes as inputs the current and the voltage at maximum power point, and the temperature
56 of the PV module. Different methods based on the Takagi Sugeno Fuzzy Rule (TSKFRBS) have been
57 described in [27 & 28].

58 The main contribution of this work is to present a new PV fault detection method based on Mamdani fuzzy
59 logic system, which can detect the defective bypass diodes and partial shading conditions. The fuzzy logic
60 system depends on three inputs:

61 2 EXAMINED PV MODULE CHARACTERISTICS

62 The PV system used in this work comprises a PV plant containing 9 polycrystalline silicon PV modules each
63 with a nominal power of 220 Wp. The photovoltaic modules are organized in 3 strings and each string is made
64 up of 3 series-connected PV modules. Using a photovoltaic connection unit which is used to enable or disable the
65 connected of any PV modules from the entire GCPV plant, each photovoltaic string is connected to a Maximum
66 Power Point Tracker (MPPT) which has an output efficiency not less than 98.5% [29]. The existing PV system
67 is shown in Figure 1a.

68 The SMT6 (60) P solar module manufactured by Romag has been used in this work. The tilt angle of the
69 PV installation is 42°. The electrical characteristics of the solar module are shown in Table 1. Additionally,
70 the standard test condition (STC) for these solar panels are: solar irradiance (G): 1000 W/m² and PV module
71 temperature (T): 25 °C.

72 Each examined PV module comprises three bypass diodes which are connected in parallel to each PV string.
73 Figure 1b shows the connection of the bypass diodes, where Figure 1c shows the junction box placed at the back
74 of the PV modules.

75 3 III. INSPECTION AND VALIDATION Method

76 In this work, the MPPT units were used to measure the voltage, and current using the internal sensors embedded
77 with this device. Subsequently, the MPPT units are connected to a Virtual instrumentation (VI) LabVIEW
78 software in order to simulate the current-voltage (I-V) curve of the examined PV modules.

79 Furthermore, the investigation of the temperature variations during partial shading and faulty bypass diodes
80 (bypass diode disconnected from the PV modules) have been captured using i5 FLIR thermal camera. This
81 camera has the following specification:

82 ? Thermal image quality: 100x100 pixels ? Field of view: 21.0 (H) x 21.0 (V)

83 ? Thermal sensitivity: 32.18 F/IV.

84 4 EXPERIMENTAL RESULTS

85 5 a) I-V curve characteristics under partial shading conditions

86 The first test will demonstrate the impact of partial shading conditions on the I-V curve for a standalone PV
87 module. The first PV module in the PV system will be covered by an opaque object to examine the PV module
88 under various partial shading conditions as shown in Figure 3a. Figure 2a and Figure 2b show the experiment
89 output for the I-V and P-V curves for all tested shading conditions. As can be noticed, while increasing the
90 percentage of shading the V_{oc} of the PV module decrease. However, the I_{sc} remains the same at 8.18 A.
91 Multiple experiments have been conducted under various partial shading conditions, starting from 10% and
92 ending up with 90%. Three thermal images of the examined PV module under partial shading conditions (10%,
93 30%, and 60%) are shown in Figure 3. In addition, all experiments were performed while there is no defective
94 bypass diodes connected in the tested PV module. As shown in Figure 4a, during 90% partial shading and no
95 disconnection of PV module bypass diodes, PV module I-V curve started to drop its I_{sc} at 18 V, we called this
96 drop as V drop in the I-V curve. However, the first drop in the I-V curve while disconnecting one bypass diode is
97 equal to 16 V. Faster drop is associated with 90% partial shading and 2 faulty bypass diodes in the PV module.

98 The last case, when all PV module bypass diodes completely removed during 90% partial shading condition.
99 In this case, the drop in the I_{sc} is obtained at the start of the I-V curve (at 0~2.87 V). This loss in the current
100 will affect the output power of the PV module significantly. The output power obtained in each case scenario is
101 presented as follows:

102 ? Furthermore, Figure 4b shows that while disconnecting one bypass diode from the examined PV module,
103 the temperature raises in the PV string associated with the faulty bypass diode location. The increase of the
104 PV sting temperature will decrease the PV output power. According to Figure 4b In order to generalize the
105 findings of the V drop , the percentage of V mpp has been compared with the V drop values, which can be
106 formalized as stated in (1) by the voltage drop percentage (PVD). As can be noticed, the regions of the PVD
107 are overlapping, and in order to increase the detection accuracy of the bypass diodes regions, the percentage of
108 open circuit voltage (POCV) is used. The POCV is calculated using ??2).

109 From the results obtained previously in Figure 4a, the POVC for each tested case scenario has been calculated
110 as the following: No fault in the bypass diodes: Disconnecting 1 bypass diode: Disconnecting 2 bypass didoes:

111 It is also worthy to mention the behavior of the I-V curves based on the measured I sc for each examined case.
112 Since I sc is another variable which could be used to examine the faulty bypass diodes in PV modules. For that
113 reason, percentage of short circuit current drop (PSCC) has been used and presented by ??3).

114 The PSCC is equal to 1 in the first 3 cases (no fault in the bypass diodes, disconnecting 1 bypass diode, and
115 disconnecting 2 bypass diodes). However, the PSCC was evaluated using partial shading conditions between 0%
116 up to 90% while disconnecting all bypass diodes in the examined PV module. The PSCC results are shown in
117 Table 2, where I-V curves are presented in Figure 5.

118 The result shows that the percentage of PSCC depends on the percentage of shading affecting the PV module.
119 An increase in the partial shading results a decrease in the PSCC percentage. (2)

120 (3)
121 V.

122 6 Proposed Fault Detection SYSTEM

123 In this section, the proposed PV bypass diode fault detection system will be presented. Firstly, the fault detection
124 system proposed in this paper is capable of detecting faults associated with bypass diodes and partial shading
125 conditions affecting the PV modules.

126 The detection system is based on the variations of the IV curve V drop , I-V curve V oc , and I-V curve I sc
127 . Next, Mamdani fuzzy logic system is used to detect the faults in the examined PV module. The general fuzzy
128 system architecture is illustrated in Figure 6.

129 Subsequently, the fuzzy system is based on three inputs:

- 130 1. PVD 2. POVC

131 7 PSCC

132 All inputs are processed by the fuzzy logic system based on the membership functions shown in Figure 7a, where
133 all the percentages are discussed previously in section IV.

134 The output of the fuzzy logic system can classify 13 different type of fault associated with PV bypass diodes
135 and partial shading conditions. Furthermore, Figure 7b illustrates the output membership function used in the
136 fuzzy system. In addition, the list of the faults are shown in Figure 7c.

137 The fuzzy logic system rule are based on: if, and statement. All selected rules in the fuzzy logic is presented
138 in Appendix A.

139 The main question related to the structure of the fuzzy logic system, that if the rules and classification could
140 be used in other PV modules? -The answer will be briefly answered next section, however, as can be seen in
141 Figure 6, the PVD, POCV and PSCC depends on the ratio of the measured and theoretical PV parameters,
142 thus, these ratios are fixed through any tested PV module. As a result of that, the fuzzy logic could be used to
143 classify the faulty bypass diodes in other PV modules as appropriate. Validate the Proposed Fault DETECTION
144 SYSTEM USING KC130GHT PV MODULE

145 In this section, the proposed fault detection system will be evaluated using a different PV module installed at
146 the University of Huddersfield, where the electrical characteristics of the PV module is shown in Table 3. Real
147 image of the PV module is shown in Figure 7. Additionally, the PV strings are connected to three bypass diodes.

148 In this section, two case scenarios will be evaluated, the first case is when the PV module under one defective
149 bypass diode, where the second case where the PV module under three defective bypass diodes.

150 8 a) PV module under one defective bypass diode and 35% 151 partial shading

152 This test was evaluated when the PV module has one defective bypass diode. The PV module output parameters:
153 V drop , V oc , and I sc are shown in Figure 9a.

154 The percentages PVD, POVC, PSCC are equal to 58.52%, 99.08% and 100%. Next, these percentages are
155 processed by the fuzzy logic system.

9 Fig. 8: Real image of KC130GHT PV module

As shown in Figure 9a, the output of the fuzzy system is equal to 1.91, which is between the region "1-2". This region indicates that there is one defective bypass diode in the PV module. In addition, the classifications of all regions are previously described in Figure 7c.

In conclusion, this test was performed by the fuzzy logic, and it has successfully detected the defective bypass diode in the PV module.

10 b) PV module under three defective bypass diodes and 65% partial shading

The second test, was performed when the PV module has three defective bypass diodes (all bypass diodes has been removed) and this test was evaluated while covering 65% of the PV module using an opaque paper. The output performance of the PV module parameters is shown in Figure 9b. The theoretical Isc dropped down to 2.81A after 0.3V. The percentage as PVD, POVC and PSCC are equal to 1.70%, 91.32%, and 35.04%.

The output of the fuzzy system is equal to 9.5, which is between the regions "9-10". This region indicates that there is 3 faulty bypass diodes and 60-70% partial shading affects the PV module.

Both tests indicate that the proposed detection system is capable of detecting the defective bypass diodes in the PV module. Subsequently, there is a high accuracy in the fuzzy logic system output results comparing to the faulty conditions affecting the examined PV module.

11 VII.

12 CONCLUSION

This paper proposed a fault detection method for PV module defective bypass diodes. The detection method is based on Mamdani fuzzy logic system, which depends on the analysis of V drop , V oc , and I sc obtained from the I-V curve of the examined PV module.

The fuzzy logic system depends on three inputs, namely percentage of voltage drop (PVD), Percentage of open circuit voltage (POCV), and the percentage of short circuit current (PSCC). The proposed fuzzy system can detect up to 13 different faults associated with defective and non-defective bypass diodes.

The detection system achieved high detection accuracy during the validation process. In addition, the fuzzy system was evaluated using two different PV modules installed at the University of Huddersfield. Finally, in order to investigate the variations of the PV module temperature during defective bypass diodes and partial shading conditions, i5 FLIR thermal camera was used.

In future, it is intended to extend the present work to detect the faults in PV bypass diodes using the analysis of the series resistance (R_s) and shunt resistance (R_{sh}) of the PV module. In addition, the fuzzy system could be replaced with artificial neural network (ANN).^{1 2}

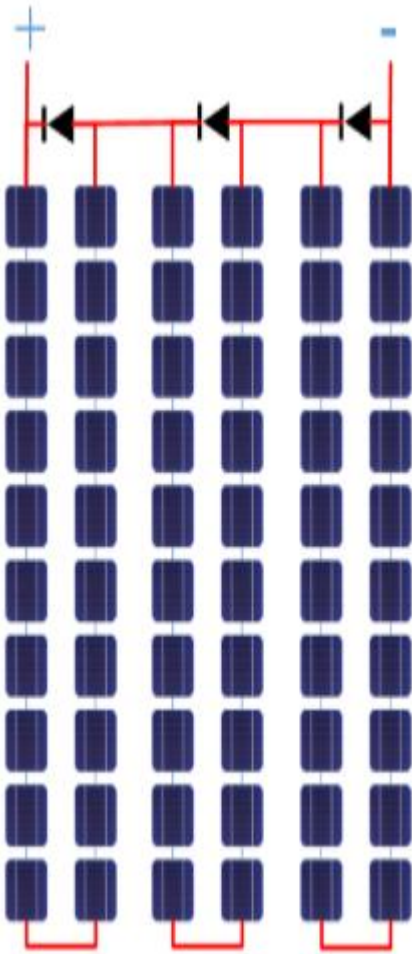
¹© 2017 Global Journals Inc. (US)

²© 2017 Global Journals Inc. (US)Global Journal of Researches in Engineering



1

Figure 1: Fig . 1 :



2

Figure 2: Fig. 2 :F

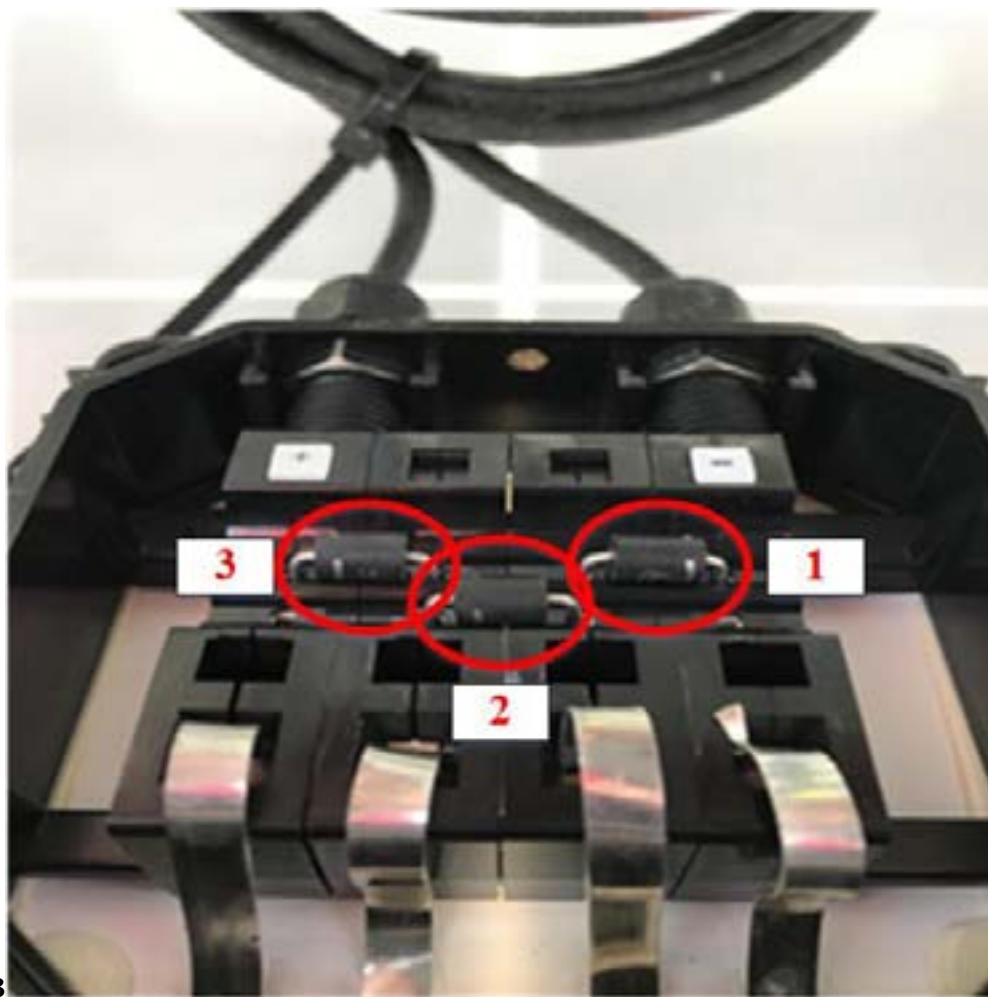


Figure 3: Fig. 3 :

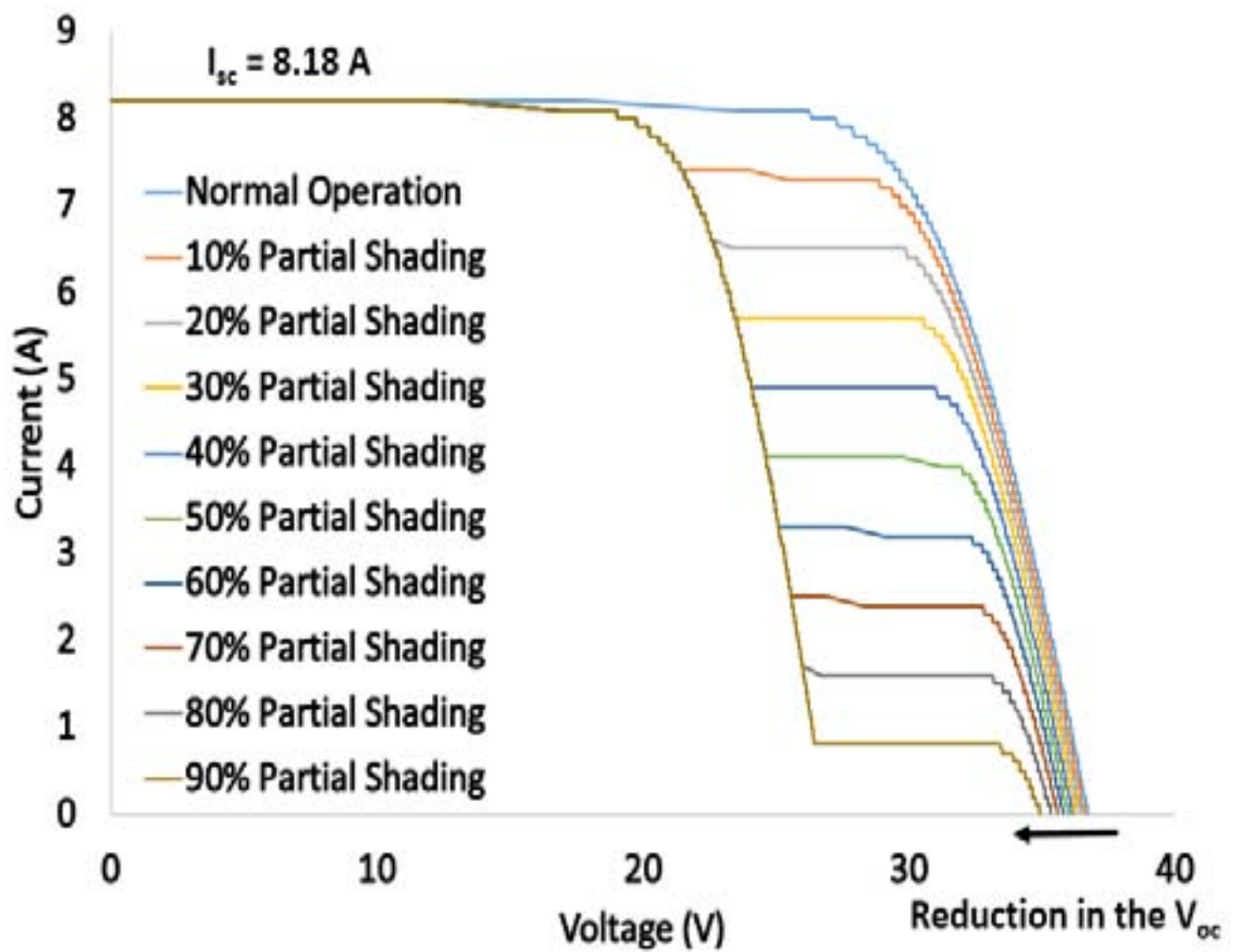
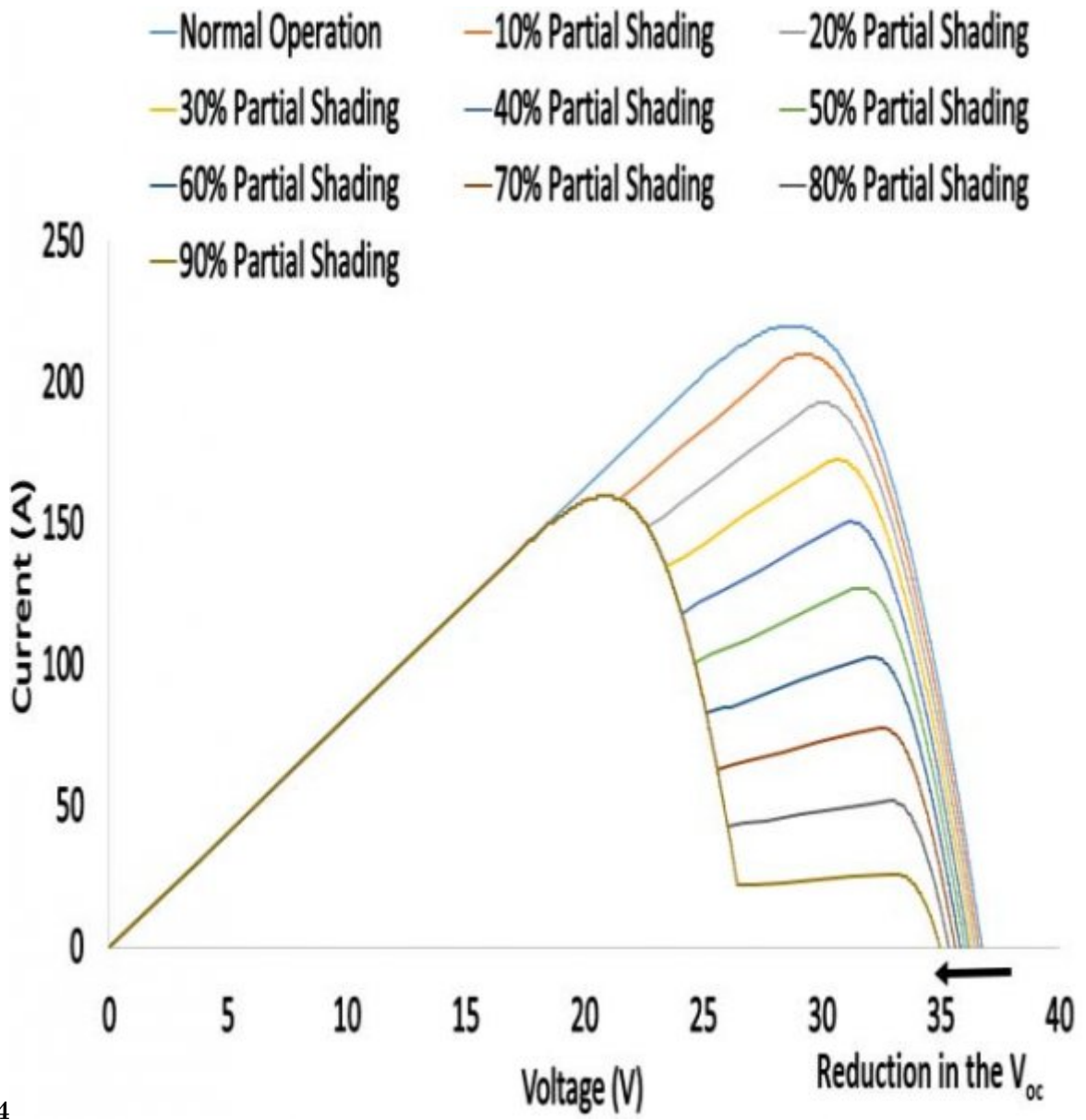


Figure 4: F



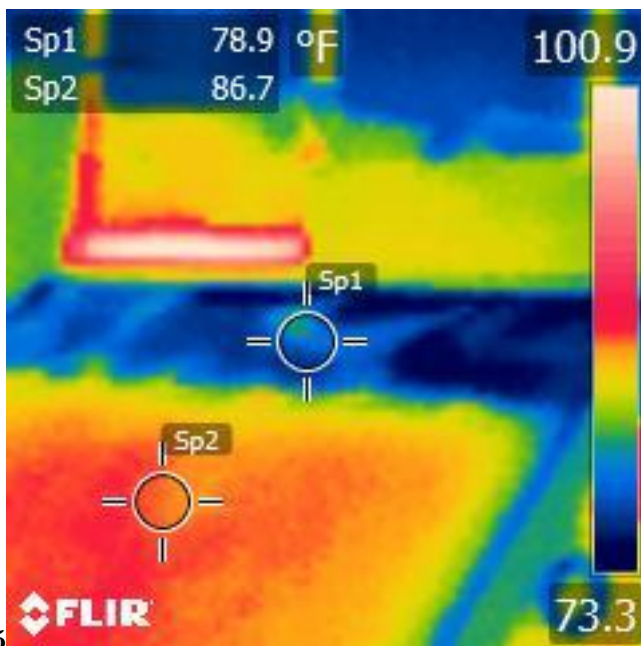
4

Figure 5: Fig. 4 :?F



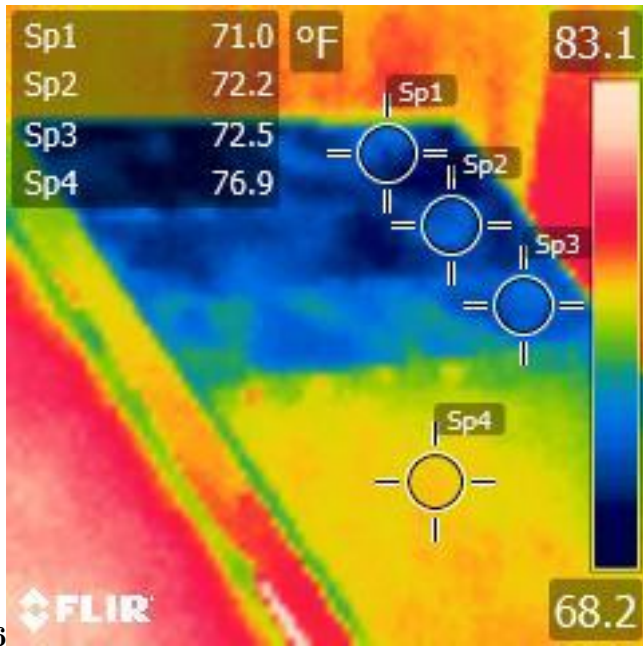
1

Figure 6: (1)



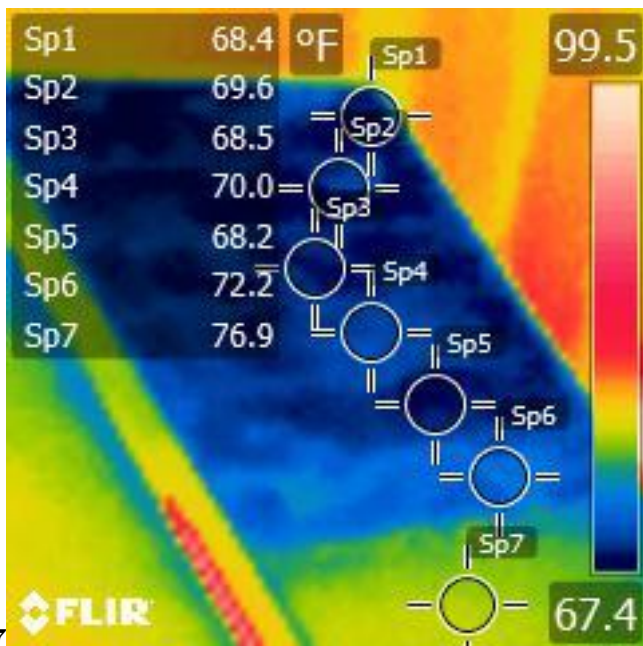
5

Figure 7: Fig. 5 :F



6

Figure 8: Fig. 6 :F



7

Figure 9: Fig. 7 :F

12 CONCLUSION



Figure 10: Fig. 9 :

1

PV module electrical characteristics	Value
Power at maximum power point (P_{mpp})	220 W
Voltage at maximum power point (V_{mpp})	28.7 V
Current at maximum power point (I_{mpp})	7.67 A
Open Circuit Voltage (V_{oc})	36.74 V
Short Circuit Current (I_{sc})	8.24 A
Number of cells connected in series	60
Number of cells connected in parallel	1

Figure 11: Table 1 :

2

Shading Percentage %	Measured Isc (A)	PSCC %
Normal Operation	8.18	100
10%	7.37	90
20%	6.55	80
30%	5.73	70
40%	4.91	60
50%	4.09	50
60%	3.28	40
70%	2.46	30
80%	1.64	20
90%	820 mA	

Figure 12: Table 2 :

3

PV module electrical characteristics	Value
Power at maximum power point (P_{mpp})	130 W
Voltage at maximum power point (V_{mpp})	17.6 V
Current at maximum power point (I_{mpp})	7.39 A
Open Circuit Voltage (V_{oc})	21.9 V
Short Circuit Current (I_{sc})	8.02 A
Number of cells connected in series	36
Number of cells connected in parallel	1

Figure 13: Table 3 :

1 Appendix A

188 Fuzzy logic system rules:

189 [Alam et al. ()] ‘A comprehensive review of catastrophic faults in PV arrays: types, detection, and mitigation
190 techniques’. M K Alam , F Khan , J Johnson , J Flicker . *IEEE Journal of Photovoltaics* 2015. 5 (3) p. .

191 [Roy et al. (2017)] ‘A Deep Learning Based Artificial Neural Network Approach for Intrusion Detection’. S S
192 Roy , A Mallik , R Gulati , M S Obaidat , P V Krishna . *International Conference on Mathematics and
193 Computing*, (Singapore) 2017. January. Springer. p. .

194 [Mallor et al. ()] *A method for detecting malfunctions in PV solar Year*, F Mallor , T León , L De Boeck , S Van
195 Gulck , M Meulders , B Van Der Meerssche . 2017. 2017.

196 [Li et al. ()] ‘An intelligent method for fault diagnosis in photovoltaic array’. Z Li , Y Wang , D Zhou , C Wu .
197 *System Simulation and Scientific Computing* 2012. p. .

198 [Ducange et al. (2011)] ‘An intelligent system for detecting faults in photovoltaic fields’. P Ducange , M Fazzolari
199 , B Lazzerini , F Marcelloni . *Intelligent systems design and applications (ISDA), 2011 11th international
200 conference on*, 2011. November. IEEE. p. .

201 [Vergura et al. ()] ‘Descriptive and inferential statistics for supervising and monitoring the operation of PV
202 plants’. S Vergura , G Acciani , V Amoruso , G E Patrono , F Vacca . *IEEE Transactions on Industrial
203 Electronics* 2009. 56 (11) p. .

204 [Detecting Defective Bypass Diodes in Photovoltaic Modules using Mamdani Fuzzy Logic System panels based on electricity prod
205 ‘Detecting Defective Bypass Diodes in Photovoltaic Modules using Mamdani Fuzzy Logic System panels
206 based on electricity production monitoring’. *Solar Energy* 153 p. .

207 [Miwa et al. (2006)] ‘Diagnosis of a power output lowering of PV array with a (-dI/dV)-V characteristic’. M
208 Miwa , S Yamanaka , H Kawamura , H Ohno . *Photovoltaic Energy Conversion, Conference Record of the
209 2006 IEEE 4th World Conference on*, 2006. May. IEEE. 2 p. .

210 [Dhimish et al. ()] *Diagnostic method for photovoltaic systems based on six layer detection algorithm*, M Dhimish
211 , V Holmes , B Mehrdadi , M Dales . 2017. 151 p. . Electric Power Systems Research

212 [Takashima et al. ()] ‘Experimental studies of fault location in PV module strings’. T Takashima , J Yamaguchi
213 , K Otani , T Oozeki , K Kato , M Ishida . *Solar Energy Materials and Solar Cells* 2009. 93 (6) p. .

214 [Saidan et al. ()] ‘Experimental study on the effect of dust deposition on solar photovoltaic panels in desert
215 environment’. M Saidan , A G Albaali , E Alasis , J K Kaldellis . *Renewable Energy* 2016. 92 p. .

216 [Saidan et al. ()] ‘Experimental study on the effect of dust deposition on solar photovoltaic panels in desert
217 environment’. M Saidan , A G Albaali , E Alasis , J K Kaldellis . *Renewable Energy* 2016. 92 p. .

218 [Dhimish and Holmes ()] ‘Fault detection algorithm for grid-connected photovoltaic plants’. M Dhimish , V
219 Holmes . *Solar Energy* 2016. 137 p. .

220 [Dhimish et al. (2017)] ‘Fault detection algorithm for multiple GCPV array configurations’. M Dhimish , V
221 Holmes , M Dales , P Mather , M Sibley , B Chong , L Zhang . *Power Tech*, 2017. June. 2017. IEEE.
222 p. .

223 [Schirone et al. ()] ‘Fault detection in a photovoltaic plant by time domain reflectometry’. L Schirone , F P
224 Califano , M Pastena . *Progress in Photovoltaics: Research and Applications*, 1994. 2 p. .

225 [Tsanakas et al. ()] ‘Faults and infrared thermographic diagnosis in operating c-Si photovoltaic modules: A
226 review of research and future challenges’. J A Tsanakas , L Ha , C Buerhop . *Renewable and Sustainable
227 Energy Reviews* 2016. 62 p. .

228 [If (PVD is 0-FaultyBypassDiode) and (POCV is 0-FaultyBypassDiode) then] *If (PVD is 0-FaultyBypassDiode)*
229 *and (POCV is 0-FaultyBypassDiode) then, (Output is 1)*

230 [If (PVD is 1-FaultyBypassDiode) and (POCV is 1-FaultyBypassDiode) then (Output is 2] *If (PVD is 1-*
231 *FaultyBypassDiode) and (POCV is 1-FaultyBypassDiode) then (Output is 2,*

232 [If (PVD is 2-FaultyBypassDiodes) and (POCV is 2-FaultyBypassDiodes) then] *If (PVD is 2-*
233 *FaultyBypassDiodes) and (POCV is 2-FaultyBypassDiodes) then, (Output is 3)*

234 [Kow et al. ()] ‘Incremental Unsupervised Learning Algorithm for Power Fluctuation Event Detection in PV
235 Grid-Tied Systems’. K W Kow , Y W Wong , R K Rajkumar , R K Rajkumar , D Isa . *9th International
236 Conference on Robotic, Vision, Signal Processing and Power Applications*, (Singapore) 2017. Springer. p. .

237 [Dhimish et al. ()] *Multi-Layer Photovoltaic Fault Detection Algorithm*, M Dhimish , V Holmes , B Mehrdadi ,
238 M Dales . 2017. (High Voltage)

239 [Bonsignore et al. ()] ‘Neuro-fuzzy fault detection method for photovoltaic systems’. L Bonsignore , M Davarifar
240 , A Rabhi , G M Tina , A Elhajjaji . *Energy Procedia* 2014. 62 p. .

12 CONCLUSION

- 242 [Silvestre et al. ()] ‘New procedure for fault detection in grid connected PV systems based on the evaluation of
243 current and voltage indicators’. S Silvestre , M A Da Silva , A Chouder , D Guasch , E Karatepe . *Energy*
244 *Conversion and Management* 2014. 86 p. .
- 245 [Ramli et al. ()] ‘On the investigation of photovoltaic output power reduction due to dust accumulation and
246 weather conditions’. M A Ramli , E Prasetyono , R W Wicaksana , N A Windarko , K Sedraoui , Y A
247 Al-Turki . *Renewable Energy* 2016. 99 p. .
- 248 [Ramli et al. ()] ‘On the investigation of photovoltaic output power reduction due to dust accumulation and
249 weather conditions’. M A Ramli , E Prasetyono , R W Wicaksana , N A Windarko , K Sedraoui , Y A
250 Al-Turki . *Renewable Energy* 2016. 99 p. .
- 251 [Lappalainen and Valkealahti ()] ‘Output power variation of different PV array configurations during irradiance
252 transitions caused by moving clouds’. K Lappalainen , S Valkealahti . *Applied Energy* 2017. 190 p. .
- 253 [Dhimish et al. ()] ‘Parallel fault detection algorithm for grid-connected photovoltaic plants’. M Dhimish , V
254 Holmes , M Dales . *Renewable Energy* 2017. 113 p. .
- 255 [If] *PVD is 3-FaultyBypassDiodes*) and, If . (PSCC is 10-20%PartialShading) then (Output is 5)
- 256 [If] *PVD is 3-FaultyBypassDiodes*) and (PSCC is 0-10%PartialShading) then, If . (Output is 4)
- 257 [If] *PVD is 3-FaultyBypassDiodes*) and (PSCC is 20-30%PartialShading) then (Output is 6, If .
- 258 [If] *PVD is 3-FaultyBypassDiodes*) and (PSCC is 30-40%PartialShading) then, If . (Output is 7)
- 259 [If] *PVD is 3-FaultyBypassDiodes*) and (PSCC is 40-50%PartialShading) then, If . (Output is 8)
- 260 [If] *PVD is 3-FaultyBypassDiodes*) and (PSCC is 50-60%PartialShading) then, If . (Output is 9)
- 261 [If] *PVD is 3-FaultyBypassDiodes*) and (PSCC is 60-70%PartialShading) then (Output is 10, If .
- 262 [If] *PVD is 3-FaultyBypassDiodes*) and (PSCC is 70-80%PartialShading) then (Output is 11, If .
- 263 [If] *PVD is 3-FaultyBypassDiodes*) and (PSCC is 80-90%PartialShading) then, If . (Output is 12)
- 264 [If] *PVD is 3-FaultyBypassDiodes*) and (PSCC is 90-100%PartialShading) then (Output is 13, If .
- 265 [Dhimish et al. ()] *Seven indicators variations for multiple PV array configurations under partial shading and*
266 *faulty PV conditions*, M Dhimish , V Holmes , B Mehrdadi , M Dales , B Chong , L Zhang . 2017. (Renewable
267 Energy)
- 268 [Dolara et al. ()] ‘Snail trails and cell microcrack impact on PV module maximum power and energy production’.
269 A Dolara , G C Lazaroiu , S Leva , G Manzolini , L Votta . *IEEE Journal of Photovoltaics* 2016. 6 (5) p. .
- 270 [Eke and Betts ()] ‘Spectral irradiance effects on the outdoor performance of photovoltaic modules’. R Eke , T
271 R Betts . *Renewable and Sustainable Energy Reviews* 2017. 69 p. .
- 272 [Kaldellis et al. ()] ‘Temperature and wind speed impact on the efficiency of PV installations. Experience
273 obtained from outdoor measurements in Greece’. J K Kaldellis , M Kapsali , K A Kavadias . *Renewable*
274 *Energy* 2014. 66 p. .
- 275 [Dhimish et al. ()] ‘The effect of micro cracks on photovoltaic output power: case study based on real time long
276 term data measurements’. M Dhimish , V Holmes , M Dales , B Mehrdadi . *Micro & Nano Letters* 2017.
- 277 [Dhimish et al. ()] ‘The Impact of Cracks on Photovoltaic Power Performance’. M Dhimish , V Holmes , B
278 Mehrdadi , M Dales . *Journal of Science: Advanced Materials and Devices* 2017.